Rene and Fokui
Journal of Electrical Systems and Inf Technol (2024) 11:1
https://doi.org/10.1186/s43067-023-00126-w

Journal of Electrical Systems and Information Technology

RESEARCH **Open Access**

Artificial intelligence-based optimal EVCS integration with stochastically sized and distributed PVs in an RDNS segmented in zones

Ebunle Akupan Rene[1*] and Willy Stephen Tounsi Fokui[2]

*Correspondence: ebunleakupanrene@gmail.com

[1] Department of Electrical and Electronic Engineering, University of Buea, P.O Box 63, Buea, Cameroon
[2] Teleconnect GmbH, 01157 Dresden, Germany

Abstract

The growing interest in electric vehicles (EVs) for transportation has led to increased production and government support through legislation since they offer environmental benefits such as reduced air pollution and carbon emissions compared to conventional combustion engine vehicles. This shift toward EV technology aligns with the goal of preserving the natural environment. To fully utilize EVs, effective management of the power grid is crucial, particularly in radial distribution network systems (RDNS) as they pose stress and deviation of power system parameters from their normal. This study proposes a novel strategy for maximizing EV utilization through EV charging stations (EVCSs) in an RDNS by considering factors such as load voltage deviation, line losses, and the presence of distributed solar photovoltaic systems at load centers. The research begins by segmenting the RDNS into zones, followed by the application of an artificial intelligence-based hybrid genetic algorithm (GA) and particle swarm optimization (PSO) approach known as hybrid GA–PSO. This approach identifies optimal locations for EVCSs integrated with photovoltaics within the network. Subsequently, the employment of individual GA and PSO algorithms to optimize EVCS placement focuses on minimizing power loss and enhancing voltage. The effectiveness of the hybrid GA–PSO algorithm is compared to that of separate GA and PSO methods. Extensive simulations using the IEEE 33-node test feeders validate the proposed techniques, demonstrating the usefulness of the hybrid GA–PSO algorithm in identifying optimal EVCS placement within each zone. The results also highlight the advantages and novelty of hybrid GA–PSO in achieving optimal EVCS placement with stochastically sized and distributed photovoltaic in an RDNS.

Keywords: Charging station, Electric vehicle, Photovoltaic, Zones, Artificial intelligence, Genetic algorithm, Optimization techniques, Particle swarm optimization, Power losses, Voltage stability margin

Introduction

The increasing interest in using electric vehicles (EVs) for transportation, particularly for passenger transport, has led to significant developments in EV production and manufacturing lines by carmakers and automobile manufacturers to meet the demand in various countries. This growth has been supported by government legislation related to EVs. A positive correlation has been observed between EV usage and environmental benefits, such as reduced air pollution levels [1] and lower carbon emissions [2]. The promotion of electric vehicles aligns with the goal of preserving the natural environment over time. Unlike traditional combustion engine vehicles that rely on fuel consumption and emit carbon dioxide [3], the advancements in power, power electronic components, and material science technology have sparked interest in different types of EV technology. The successful integration of EV charging stations into the power grid is crucial for achieving system stability and accommodating the load changes associated with EV charging.

EVs are gradually rendering conventional automobiles obsolete [4]. However, the question of charging infrastructure poses a level of uncertainty and concern among many people. Unlike stationary electrical equipment, EVs are primarily in motion. Therefore, it is crucial to have accessible charging facilities available after each use, enabling EVs to be utilized anywhere and at any time. Consequently, research focuses on various experimental settings, including solid-state batteries, magnetic batteries, and lithium batteries, which are integral to battery technology [5]. Battery technology plays a critical role in determining the size and range of EVs. Consequently, the development of batteries presents its own challenges, with extensive research efforts dedicated to reducing charging time and increasing power density. Additionally, motor technology in electric vehicles plays a vital role in their traction driving capabilities, and its efficiency is determined by the amount of energy the motor can draw from the EV's batteries [6]. Battery technology and motor technology are distinct yet interconnected fields of study, often explored in conjunction with materials technology.

Researchers have also examined the impact of EVs on the electrical power system, specifically power system losses, node voltage stability, power system oscillations, energy demand response, and optimal charging station deployment [7, 8]. Due to the influence of EVs on electricity consumption, optimization strategies are necessary to replicate ideal conditions and enable effective energy planning to ensure grid reliability. Consequently, energy management sources need to be investigated alongside the selection of efficient electric car chargers to effectively utilize different energy sources during the EV charging process. Currently, photovoltaic (PV) power plants are receiving significant attention as potential energy sources [9]. PV systems can be integrated into radial distribution network systems (RDNSs) to reduce overall power losses in the electrical power system [10]. A step-down power transformer is utilized to connect the EV charging equipment to the RDNS, enabling the high voltage from the system to be adjusted to a manageable level. Additionally, charging EVs at home typically involves connecting the power cord to a home charger.

The electric vehicle load is a major consumer of energy from the grid. Various load models, such as power constant (P) load, current constant (I) load, polynomial load, *Z–I–P* load, and voltage source converter models, have been defined to represent electric vehicle loads [11]. Large-scale EV charging stations (EVCSs) significantly impact the electrical power grid, necessitating grid enhancements [11]. Several studies have demonstrated the adaptability of the electrical power system to address these challenges. Genetic algorithms (GAs) are widely used optimization techniques for effectively allocating distributed generators (DGs) [12, 13]. Researchers in [14] and [15] have, respectively, proposed single- and multi-objective optimization strategies using quantum particle swarm optimization (PSO) for grid frequency control and GA and PSO for determining the size and location of multiple DGs within RDNS, considering different load models. Another study proposed a hybrid bacterial foraging optimization algorithm and PSO (BFOA–PSO) approach to optimize the placement of EVCSs in distribution networks with high penetration of rooftop PV systems [16]. The optimization problem considers minimizing power losses, voltage deviation, and maximizing voltage stability. Consideration of the inductive nature of PV converters was also addressed in another study using a hybrid GA–PSO approach for optimal allocation of plug-in EV charging stations (PEVCS) in distribution networks with high volumes of distributed generation [17]. These studies highlight the importance of load models and the integration of renewable energy sources in determining optimal EVCS placements. The author [16, 17] had considered the distribution network to be a module, and EVCS could be placed anywhere without considering the sparsity of the load distribution.

This paper introduces a novel strategy for the optimal placement of EVCSs and distributed PV systems in an RDNS. The strategy involves dividing the RDNS into zones using improved spectral clustering and utilizing individual GA, PSO, and hybrid GA–PSO approaches to determine optimal EVCS placements within each zone. Separate GA, PSO, and hybrid GA–PSO techniques are employed to size and position the distributed PV systems, assessing their impact on power loss and voltage dips caused by EVCSs. The goal is to identify the most cost-effective settings for deploying EVCSs in an RDNS with randomly placed PV systems, utilizing the hybrid GA–PSO approach to leverage the strengths of both GA and PSO methods. The paper also presents an introduction to the current state of electric vehicles (EVs) and their impact on the environment and transportation. It discusses the challenges associated with EV charging infrastructure and the advancements in battery and motor technologies. It also highlights the research efforts focused on the impact of EVs on the electrical power system and the optimization strategies for efficient energy management and grid reliability. Overall, the paper aims to provide insights into the challenges and developments in EV technology, EV charging infrastructure, and optimization strategies for efficient energy management in the context of EVs.

The paper is organized as follows: It formulates the mathematical model and optimization methods for selecting optimal EVCS locations in network zones with distributed PV systems. It then presents simulation results of optimal EVCS and PV placements obtained using PSO, GA, and hybrid GA–PSO optimization techniques. The paper concludes with a final section summarizing the findings and potential for the proposed method.

Methodology

The methodology used in this research focuses on minimizing the impact of increased penetration of EVCSs and distributed generators (PV systems) on the performance of the distribution system. Traditional load flow methods like Newton–Raphson and Guass–Seidel are not suitable for accurate results. Instead, an efficient load flow method based on the forward–backward approach, as described in [18], is employed. The study aims to achieve three objectives: minimizing power losses, reducing voltage variation, and improving the voltage stability index of the network.

Distribution network modeling

Electric vehicles are direct current consumption load that is charged through the grid. Based on certain conditions of the grid, the EV can also be discharged through the grid. However just the former has been considered in this paper, and thus the electric charging stations are seen as direct current loads to the grid's RDNS. The IEEE 33-bus system is the selected use-case network in this study. The RDNS is broken up into zones so that each zone can have an EVCS with a number of charging spots to serve its own needs. This RDNS is large and balanced at a voltage of 12.66 kV as shown in Fig. 1.

Modeling of the number of EVs and charger type

The number of homes in the research region must be known in order to get an accurate estimate of the total EV population in each area. In this work, each family has been constrained to have a total apparent power (S') requirement of 12.7kVA. Based on this consideration, the total number of homes (N) in each zone can be estimated using Eq. (1), assuming a load factor of unity [17].

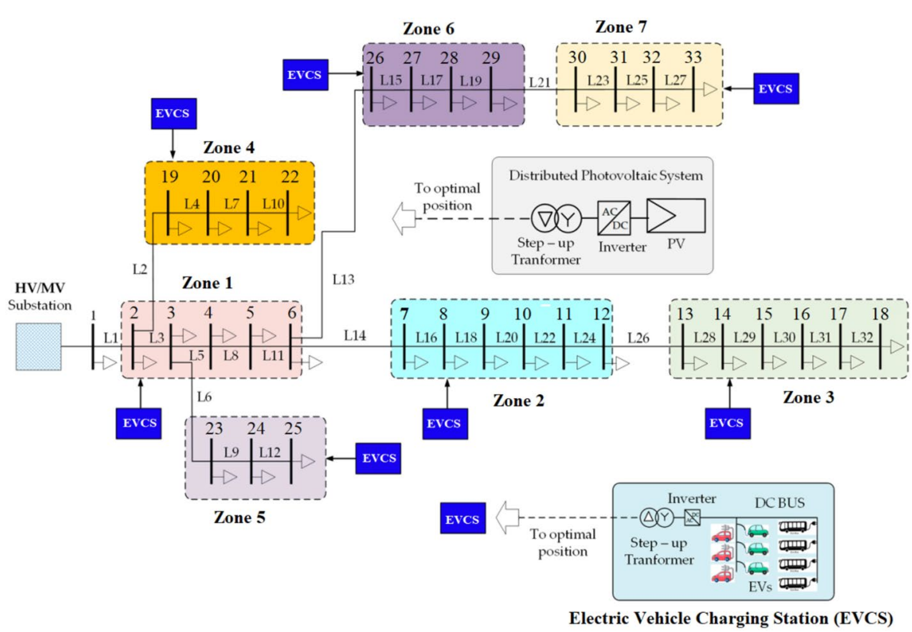

Fig. 1 Test bus system segmented into seven zones

Table 1 Estimated number of homes and EVs in each zone

Zones	Total power of each zone, *S*-kVA	Power demand by each home, *S*-kVA	No. of homes, *N*	Power demand of residential load	No. of EVs in each zone, *n*
1	487.6474	12.7	39	390.1179	11
2	695.4495	12.7	55	556.3596	16
3	494.4947	12.7	39	395.5958	11
4	393.9543	12.7	31	315.1634	9
5	1033.1505	12.7	82	826.5204	24
6	331.0589	12.7	27	264.8471	8
7	1020.0490	12.7	81	816.0392	24
Total number of EVs					**103**

Table 2 A selection of EVs and their charging systems features [16]

EV model	EV specification	Charging type			
		Level 1 (11 kW)		Level 2 (22 kW)	
		Charging time	Quantity	Charging time	Quantity
Nissan Leaf 2018	36 kWh, 220 km	11 h30 m	10	6 h30 m	9
Renault Zoe ZE50 Ri10	53 kWh, 3 15 km	5 h45 m	15	3 h	11
Honda e	28.5 kWh, 170 km	9 h15 m	12	5 h15 m	9
MG ZS EV	42.5 kWh, 220 km	13 h30 m	7	7 h45 m	9
Mazda MX 30	30 kWh, 170 km	9 h 45m	12	5 h30 m	9
Total number of EVs	56		47		

$$N = \frac{S}{S'} \tag{1}$$

where S is the total apparent power in the study area. The number of homes and EVs in each zone is shown in Table 1 after the calculation. The RDNS has been thought of as a residential and commercial network with residential loads accounting for 80% of the total load in each zone.

Equation (2) can be used to figure out the number of EVs, n if the rate of EV integration (%EV) is known. A percentage of EV penetration of 30% maximum for the test bus network has been considered. Using Eq. (2), the total number of EVs found in the research area is 103.

$$\%\mathrm{EV} = \frac{n}{N} * 100 \tag{2}$$

This study looks at five different EV models. The features and charger specifications of the five different types of EVs are listed in Table 2, along with the corresponding amounts. Both the level 1 and level 2 type chargers are well-suited with these types of EVs.

Table 3 EVCSs with both level 1 and level 2 CPs

Charger type	Rating CPs *P*-kW	No. of CPs per EVCS	Rating of EVCS, *P*-W	Rating of EVCS, *Q*-kVAR	No. of EVCS	Total rating of EVCS, *S*-kVA
Level 1	11	28	308	149.17	4	1368.89
Level 2	22	25	550	266.38	3	1833.34

Number of EV charging points and EVCS power capacity

Seven EVCSs are placed around the RDNS divided into zones in a way that stores energy for the 103 EVs. In this study, both level 1 and level 2 chargers with a specific number of charging points (CPs) have been considered, which are listed in Table 3, and were used. At a power factor of 0.90, EVCSs that have constant outputs are used. This had been thought of as a way to deal with the fact that the converters at the CPs use a lot of reactive power. The following equation defines how the EVCS' reactive power Q_{EVCS} is computed for a chosen active power P_{EVCS} for a given power factor angle φ_{EVCS}

$$Q_{\mathrm{EVCS}} = P_{\mathrm{EVCS}} * \tan\varphi_{\mathrm{EVCS}} \tag{3}$$

Modeling of distributed randomly sized PVs

In order to integrate the reactive power injection capabilities of the voltage source inverters utilized in grid-connected PV systems, the PV systems are modeled as negative loads in this work. PV systems have a penetration rate of 35%. Although there are numerous methods for estimating PV penetration levels, the percentage of PV penetration may be derived as the ratio [16]:

- the ratio of total PV system output to total generation
- Peak PV capacity to peak apparent power of loads
- PV-rated power to the active power demand of loads

The last option for calculating PV penetration percentage is used to compute the total PV-rated power needed at 35% penetration, which is 1105.17 kW for the test network given that the total load demand of the network is 3157.75 kW [19]. As a result, with a power factor of 0.95, the PV systems inject 363.25 kVAR into the test network. The equation below defines how the PV reactive power Q_{PV} injected is computed from its active power P_{PV} for a given power factor angle φ_{PV}

$$Q_{\mathrm{PV}} = P_{\mathrm{PV}} * \tan\varphi_{\mathrm{PV}} \tag{4}$$

The dispersed PV systems are randomly sized with each PV system made up of 1 kW PV modules. This allows for the PV systems to be arbitrarily sized and located over the network. The random function generates random nodes, which are used to allocate the 1 kW PV modules to be installed on each target node. Using Eq. (5), the overall PV power rating throughout the network is made to be 1105.17 kW.

$$n_k = \frac{rand(k)}{\sum_{k=2}^{33} rand(k)} * N_T \tag{5}$$

where n_k is the number of PV modules on node k, k is the load node number, with $k = 2$ being the first load node in the network, $rand(k)$ is a random generator responsible for selecting random values between 0 and 1 and allocating them to node k, and N_T is a cautiously chosen number such that the total PV capacity in the network is constant. From Eq. (6), the PV capacity for each load node can be calculated.

$$P_{\mathrm{pv}_k} = n_k * P_{\mathrm{pv}_r} \tag{6}$$

where P_{pv_k} denotes the PV capacity at node k and P_{pv_r} denotes the rating (1 kW) of a single PV. As a result, the total power rating P_{pv_T} of distributed PV systems is given by Eq. (7).

$$P_{\mathrm{pv}_T} = \sum_{k=2}^{33} P_{\mathrm{pv}_k} \tag{7}$$

EVCS location and placement

When connecting EVCSs to an RDNS, the operational conditions undergo significant changes compared to the base case configuration. Planning EVCS installations requires careful consideration of various factors, including the most effective techniques, the number and capacity of EVCS units, optimal installation locations, and appropriate connection types.

It is crucial to exercise caution when determining the best EVCS locations in a distribution network. Suboptimal placements can lead to increased system losses and higher costs. Studies indicate that placing EVCSs in unsuitable or inappropriate locations can result in even higher system losses than those already present in the network [20]. The challenge at hand involves strategically positioning seven EVCSs within the IEEE 33-bus system, which is populated with randomly sized and distributed PV systems accounting for 35% of the total load demand.

Problem formulation

Deploying EVCS in an RDNS has several benefits, including reduced line loss, improved voltage stability, enhanced network reliability, and increased security. However, determining the optimal placement of EVCS involves solving a nonlinear optimization problem with objective functions and constraints related to power balance, voltage, and current. The proposed solution aims to minimize peak load power loss and voltage variation while enhancing voltage stability in the RDNS. Thus, the multi-objective function is mathematically expressed in this case as follows:

$$\check{J}^* = \text{Minimum}\left\{\check{J}_1, \check{J}_2\right\} \tag{8}$$

where $\check{J}_1$ and $\check{J}_2$ correspond, respectively, to the total power loss and the voltage deviation index. The following is a description of the mathematical equation that represents the multi-objective function.

(1) Modeling of the objective function

(i) Real and reactive power losses

By strategically placing EVCSs in the distribution network, instability caused by peak loading situations can be mitigated, ensuring that constraints are not violated. This optimal EVCS placement minimizes power loss while adhering to the limits of system constraints. The precise branch loss for the distribution system can be obtained using equation, [21] (7).

$$\begin{cases} S_{ik}^{\text{kW Loss}} = \left(\left| \check{V}_i - \check{V}_k \right|^2 \left| \check{Y}_{ik} \right| \cos \gamma_{ik} \right) \\ S_{ik}^{\text{kWAR Loss}} = \left(\left| \check{V}_i - \check{V}_k \right|^2 \left| \check{Y}_{ik} \right| \sin \gamma_{ik} \right) \end{cases} \tag{9}$$

where $S_{ik}^{\text{kW Loss}}$ and $S_{ik}^{\text{kVAR Loss}}$ are the total real and reactive powers losses from bus i to bus k respectively, $\check{V}_i$ and $\check{V}_k$, respectively, represent the voltage of bus i and k, $\check{Y}_{ik}$ and γ_{ik} represent, respectively, the admittance and the admittance angle of the line between bus i and bus k. Therefore, the function for the minimum amount of total power loss is given as:

$$\check{J}_1^* = \text{Min} \sum_{i=1}^{n} \sum_{k=1}^{n} \left(S_{ik}^{\text{kW Loss}} + S_{ik}^{\text{kVAR Loss}} \right), \quad i \neq k \tag{10}$$

where n is the total number of buses in the network.

(ii) Voltage deviation index (VDI)

The main focus is controlling the voltage profile of the RDNS when incorporating EVCSs. The voltage profile undergoes changes due to the inclusion of EVCSs in the distribution system. Each bus in the RDNS can be analyzed individually. To ensure voltage stability, it is important for the EVCS to minimize the voltage gap between the normal bus voltage and the rated bus voltage. Equation (11) describes the equation for calculating the required voltage deviation, which represents the deviation of bus voltage magnitudes from the reference voltage magnitude [22].

$$\check{J}_2^* = \text{Min} \sum_{j=1}^{n} \left(1 - \frac{\check{V}_j}{\check{V}_{\text{REF}}} \right)^2 \tag{11}$$

where $\check{V}_j$ represents the voltage at bus j, $\check{V}_{\text{REF}}$ is the slack bus voltage and n represents the number of buses. In light of this, transforming Eqs. (10) and (11) into a minimization function results in the mathematical formulation of a multi-object function represented in Eq. (12)

$$\check{J}^{*} = \left\{ \beta_1 * \check{J}_1^{*} + \beta_2 * \check{J}_2^{*} \right\} \tag{12}$$

where β_1 and β_2 represent some hyperparameters to enhance the objective and they have been carefully chosen.

(2) Modeling constraints

(i) Equality constraints

The power requirement constraints in the system are determined by the power balance equation, which ensures that the power supplied by the EVCS meets both the system demand and internal losses. The equation for calculating the power balance can be derived from Eqs. (13) and (14) [17].

$$P_{\mathrm{G}} + \sum P_{\mathrm{PV}} = \sum P_{\mathrm{L}} + \sum P_{\mathrm{EVCS}} + \sum P_{\mathrm{LOSS}} \tag{13}$$

$$Q_{\mathrm{G}} + \sum Q_{\mathrm{PV}} = \sum Q_{\mathrm{L}} + \sum Q_{\mathrm{EVCS}} + \sum Q_{\mathrm{LOSS}} \tag{14}$$

where P_{G} and Q_{G} are the real and reactive power from the grid, P_{PV} and Q_{PV} are the real and reactive power from the PV system, P_{L} and Q_{L} are the real and reactive power demands, P_{EVCS} and Q_{EVCS} are the real and reactive power demand by a single EVCS, and P_{LOSS} and Q_{LOSS} are the real and reactive power losses.

(ii) Inequality constraints

To ensure compliance with the distribution system's limits, several factors need to be considered: The maximum power generated by the PV system should not surpass the permissible limits, voltage variation should be kept below 5%, and the number of charging points (CPs) and charging stations (CSs) should fall within the allowable minimum and maximum values.

- *Voltage constraint:* The voltage magnitude $\left|\check{V}_j\right|$ of each bus must adhere to predefined limits as specified by the following equation.

  $$\left|\check{V}_j\right|^{\mathrm{m}} \leq \left|\check{V}_j\right| \leq \left|\check{V}_j\right|^{\mathrm{M}}; \quad 0.95 \leq \left|\check{V}_j\right| \leq 1.05$$

  where $\left|\check{V}_j\right|^{\mathrm{m}}$ and $\left|\check{V}_j\right|^{\mathrm{M}}$ are the voltage minimum and maximum at bus j.
- *Voltage angle constraints:* The voltage angle δ_j of each bus must fall within the predefined limits defined by the following equation.

  $$\delta_j^{\mathrm{m}} \leq \delta_j \leq \delta_j^{\mathrm{M}}$$

  where δ_j^{m} and δ_j^{M} are the minimum and maximum voltage angle at bus j.

- *PV power constraints:* The real power P_{pv_j} and reactive power Q_{pv_j} limits of the PV system at bus j are primarily determined by the power factor (0.95) and the maximum permissible bus capacity.

  $$P_{\mathrm{pv}_j}^{\mathrm{m}} \le P_{\mathrm{pv}_j} \le P_{\mathrm{pv}_j}^{\mathrm{M}} \text{ and } Q_{\mathrm{pv}_j}^{\mathrm{m}} \le Q_{\mathrm{pv}_j} \le Q_{\mathrm{pv}_j}^{\mathrm{M}}$$

  where $P_{\mathrm{pv}_j}^{\mathrm{m}}$ and $P_{\mathrm{pv}_j}^{\mathrm{M}}$ define the PV real power minimum and maximum at bus j and $Q_{\mathrm{pv}_j}^{\mathrm{m}}$ and $Q_{\mathrm{pv}_j}^{\mathrm{M}}$ define the PV reactive power minimum and maximum at bus j.
- *Current constraint:* The distribution feeder current limit I_{rated} should be kept within the rated limit.

  $$I_{\mathrm{rated}} \le I_{\mathrm{rated}}^{\mathrm{M}}$$

  where $I_{\mathrm{rated}}^{\mathrm{M}}$ is the maximum rating of the distribution feeder.
- *Charging power constraints:* The charging power P_{EVCS_j} of each EVCS at bus j must be within predefined limits.

  $$P_{\mathrm{EVCS}_j}^{\mathrm{m}} \le P_{\mathrm{EVCS}_j} \le P_{\mathrm{EVCS}_j}^{\mathrm{M}} \text{ and } Q_{\mathrm{EVCS}_i}^{\mathrm{m}} \le Q_{\mathrm{EVCS}_i} \le Q_{\mathrm{EVCS}_i}^{\mathrm{M}}.$$

  where $P_{\mathrm{EVCS}_j}^{\mathrm{m}}$ and $P_{\mathrm{EVCS}_j}^{\mathrm{M}}$ define the EVCS real power minimum and maximum at bus j and $Q_{\mathrm{EVCS}_j}^{\mathrm{m}}$ and $Q_{\mathrm{EVCS}_j}^{\mathrm{M}}$ define the PV reactive power minimum and maximum at bus j.
- *Charging point constraints:* The number of charging points $\mathrm{CP_j}$ of each EVCS at bus j must be within specified margin.

  $$\mathrm{CP}_j^{\min} \le \mathrm{CP}_j \le \mathrm{CP}_j^{\max}$$

  where $\mathrm{CP}_j^{\min}$ and $\mathrm{CP}_{\mathrm{j}}^{\max}$ are the minimum and maximum number of charging points at bus j.
- *Charging station constraints:* The number of EVCSs must be within the margins.

  $$CS^{\min} \le \mathrm{CS} \le \mathrm{CS}^{\max}$$

  where $\mathrm{CS}^{\min}$ and $\mathrm{CS}^{\max}$ are the minimum and maximum number of charging stations in the distribution network.
- *Line loading constraints:* The rating S of the distribution line must be respected.

  $$S \le S^{\mathrm{M}}$$

  where S^{M} is the maximum rating of the distribution line.

Study of algorithm

Optimal placement of EVCSs with random penetration of PV systems is a multi-objective constrained optimization problem. This study solves EVCS placement using a unique GA–PSO to demonstrate the effectiveness of hybrid GA–PSO over individual GA and PSO. In order to assess how well the proposed algorithms address the problem of EVCS location and placement in a segmented RDNS, the IEEE 33-bus test system has been has been used. The 33-bus system has 32 branches and can handle a combined capacity of 3.72 MW and 2.30 MVAR. The line and load data for the 33-bus test system are available in [19].

(a) Particle swarm optimization (PSO)

PSO (particle swarm optimization) is an artificial intelligence technique used to solve problems in n-dimensional spaces. It leverages individual and collective experiences to guide decision-making. PSO was developed by James Kennedy and Russell Eberhart in 1995, inspired by the behavior of birds in groups studied by Frank Heppner [23, 24]. In PSO, a swarm of randomly selected agents/particles represents potential solutions. Each particle has a random speed and explores the search space. They remember their best position (X_B) and associated fitness. The swarm's overall best position is called the global best (X_G). In an n-dimensional space, each particle's position is represented as $X_k = [x_{k1}, x_{k2}, ..., x_{kn}]$. The velocity of particle k is denoted as $X_k = [x_{k1}, x_{k2}, ..., x_{kn}]$. The particles' movement is governed by velocity and position equations at the Tth iteration defined by Eqs. (15) and (16), respectively [14].

$$V_k^{T+1} = \omega^T V_k^T + C_1 R_1^T \left(X_{B_k} - X_k^T \right) + C_2 R_2^T \left(X_G - X_k^T \right) \tag{15}$$

$$X_k^{T+1} = X_k^T + V_k^{T+1} \tag{16}$$

where $k = 1, 2, ..., N_p$, where N_p denotes the swarm size; ω^T denotes inertia weight at iteration T; and C_1 and C_2 are two positive constants denoted as the cognitive and social parameters, respectively; and R_1^T and R_2^T are random values uniformly distributed in a range [0, 1]. At each iteration, Eq. (15) is used to calculate the kth particle's new velocity, V_k^{T+1}, while Eq. (16) calculates the kth particle's new location, X_k^{T+1} by adding its new velocity, V_k^{T+1} to its previous position, X_k^T

(b)Genetic algorithm (GA)

Genetic algorithms (GAs) are a prominent metaheuristic technique for solving highly nonlinear computational problems [25]. They are inspired by natural selection and genetics, operating on string structures called chromosomes. GAs develop an initial population into a population of high-quality individuals representing solutions to the problem. The fitness function evaluates the quality of each individual based on a specific criterion. Selection, crossover, and mutation are the main genetic operators applied to individuals in each generation. Selection chooses elite individuals as parents using fitness values; crossover combines genetic material from parents to produce offspring, and mutation introduces random modifications to the chromosome [26]. In summary, GA is a trending optimization algorithm that uses selection, crossover, and mutation to evolve a population toward high-quality solutions.

A number of papers on the hybridization of PSO with other heuristic optimization approaches have been published; notably, the hybrid approach of PSACO (particle swarm ant colony optimization) is suggested by Sheloker et al. [27] for extremely nonconvex optimization problems. Another is the paper published in 2008 [28] by Kao and Zahara for global optimization of multimodal functions which implemented GA with PSO as a hybrid approach. However, the application of the GA–PSO hybrid model in advanced optimization and control strategies is currently limited. Therefore, the focus of the present study is to develop an optimal placement technique using a hybrid GA–PSO model. This technique aims to place EVCSs in an RDNS divided into zones.

(c) Hybrid GA–PSO algorithm

According to the literature [29, 30], most evolutionary approaches use the following procedure:

1. An initial population is generated at random.
2. Determine the fitness value for each particle based on the best distance.
3. Fitness values define population reproduction.
4. Stop if optimum solutions are discovered. Otherwise, create a new generation of population and go to 2.

PSO and GA share some similarities in their processes. Both start with a randomly generated population and use fitness values to evaluate the population. They also make modifications to the population and apply random procedures to search for the best solution. However, neither approach guarantees success. One key difference is that PSO lacks genetic operators like crossover and mutation. In PSO, particles update themselves based on their intrinsic velocity, while GA uses chromosomes to transfer information. PSO tends to converge to the optimal solution more quickly than GA, even in the local version.

The proposed hybrid GA–PSO approach aims to combine the strengths of both algorithms. It merges the two algorithms, with the optimal solution derived from PSO further improved by GA through the use of selection, crossover, and mutation operators. This hybrid approach aims to increase exploitation using PSO and exploration using GA, resulting in improved performance. The flowchart diagram of the hybrid GA–PSO is seen in Fig. 2.

Simulation

In some cases, users are not only interested in improving the performance of a model but also in reducing the associated expenses related to its features [31]. The cost of a feature can be measured in terms of economy, time, or other resources required to obtain objective values [32, 33]. Additionally, computational issues can also contribute to the cost [34]. In this study, a single fitness function is used to minimize both power loss and voltage deviation. The simulation settings for the GA–PSO algorithm are presented in Table 4. MATLAB is employed for conducting simulations under high-load conditions, where all EVCSs are connected and charging, and PV systems are operating at their peak output. The test network used is the 33-bus test feeder, which is segmented into zones. The GA–PSO algorithm is utilized to determine the optimal placement of an EVCS in

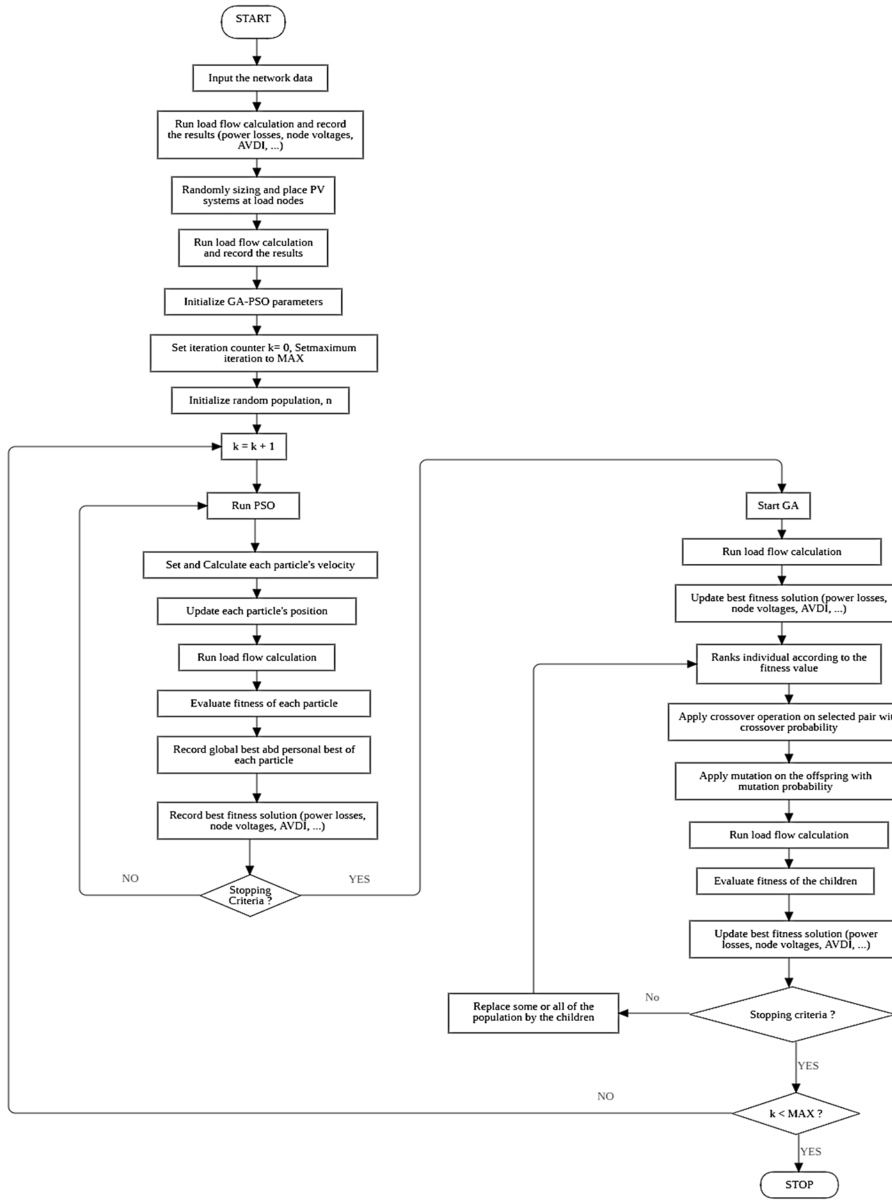

Fig. 2 Flowchart of hybrid GA-PSO

Table 4 GA–PSO parameters

Parameter	Symbol	Value
Population size	n_{POP}	30
Number of iterations	T	20
Inertia coefficient	ω	1
Personal learning coefficient	C_1	2
Social learning coefficient	C_2	2
Crossover and mutation probabilities	Pc, pm	1, 0.02

Table 5 EVCSs and randomly sized and distributed PVs best locations with hybrid GA–PSO

Charger type	Zones	No. of executions of algorithm							
		Eexcution-1		Eexcution-2		Eexcution-3		Eexcution-4	
		EVCS location	PV location	EVCS location	PV location	EVCS location	PV location	EVCSs location	PV location
Level 1	Zone-1	5		4	3	3	4	4	
	Zone-2	9	10,12	9	8,19,11	8	10,11,12	8	8,10,11,12
	Zone-3	15	14,15,18	15	13,15,16	15	13,15,18	16	14,16,18
	Zone-4	22		21		21		22	
Level 2	Zone-5	25		24		25		24	
	Zone-6	27	27,28	27	26,28	28	27	29	27,29
	Zone-7	32	31,32,33	33	31,32,33	33	30,32,33	33	31,32

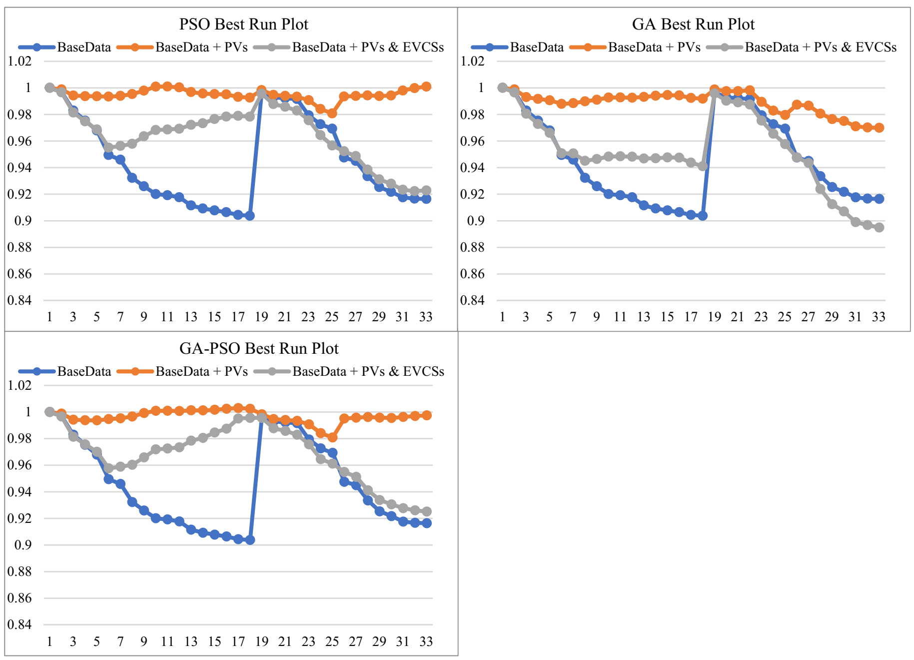

Fig. 3 Voltage profile under best test cases for PSO, GA, and GA–PSO

each zone. The chosen parameters are carefully selected to ensure both speed and accuracy in the solution process. The proposed technique has been designed to provide an improved version of the findings in [16, 17].

Results and discussion

Because the study is concerned with randomly sized and placed PV systems, four cases of stochastically sized and sited PV systems are taken into account for optimal EVCS placement. The EVCSs are optimally placed in each case using the hybrid GA–PSO optimization technique, and the results are recorded. Furthermore, the EVCSs are optimally placed using GA and PSO separately. This is required to validate the efficacy of the proposed hybrid GA–PSO compared to individual GA and PSO used in locating the best locations for the EVCSs in the distribution network with randomly sized and placed distributed PV systems.

Optimal placement of EVCSs and penetrated PV systems

Table 5 presents the optimal allocation of EVCSs for each zone and the randomly distributed photovoltaic systems in each simulation scenario. The hybrid GA–PSO algorithm was employed to test the placement of stochastically sized and located PV systems under various execution cases. The table illustrates the best positions and PV sites determined by the GA–PSO algorithm for EVCSs in each case.

In the subsequent sections, we will examine the impact of integrating EVCSs into the test network with distributed PV systems and how this integration has influenced the overall network performance.

Bus voltage profile

In Fig. 3, the network voltage profiles for all simulation conditions are given. It has been found that the random insertion of PV systems into the RDNS at a penetration level of 35% leads to a general improvement in the voltage profile of the RDNS from the base case.

The improvement in network performance can be observed across all three algorithms when considering random penetration of PV systems. Linking the PV systems at load centers has led to an enhancement in the network's voltage profile. This improvement is attributed to the PV systems being connected in close proximity to the load demand, reducing reliance on the grid. To maintain the improved voltage profile, it is important to strategically distribute the EVCSs in a manner that minimizes disruptions. The GA–PSO algorithm identifies optimal locations for EVCSs in each zone, ensuring that the increased loads from EVCSs do not significantly alter the voltage levels at network nodes. This holds true for all four cases, considering random sizing and placement of PV systems.

Comparing the simulation results, the hybrid GA–PSO approach outperforms the individual GA and PSO algorithms. The minimum voltage achieved by hybrid GA–PSO is 0.92511 p.u., while the individual GA and PSO algorithms yield lower values of

Table 6 Compared network's voltage when EVCSs and PVs are placed using PSO, GA, and hybrid GA–PSO

Base case	**Minimum node voltage under different executions (pu)**					
Vmin: 0.90378	**PSO**		**GA**		**GA–PSO**	
Vmax: 1	**Vmin**	**Vmax**	**Vmin**	**Vmax**	**Vmin**	**Vmax**
Execution-1	0.90792	1	0.89979	1	0.92411	1
Execution-2	0.92258	1	0.92814	1	**0.92511**	1
Execution-3	**0.92233**	1	0.91695	1	0.92214	1
Execution-4	0.9214	1	**0.89494**	1	0.92278	1
Min voltage	**0.90792**		**0.89494**		**0.92214**	

Bold value indicates the best minimum voltage values for each execution considering PSO, GA, GA–PSO and also the overall best voltage minimum value for each PSO, GA, GA–PSO

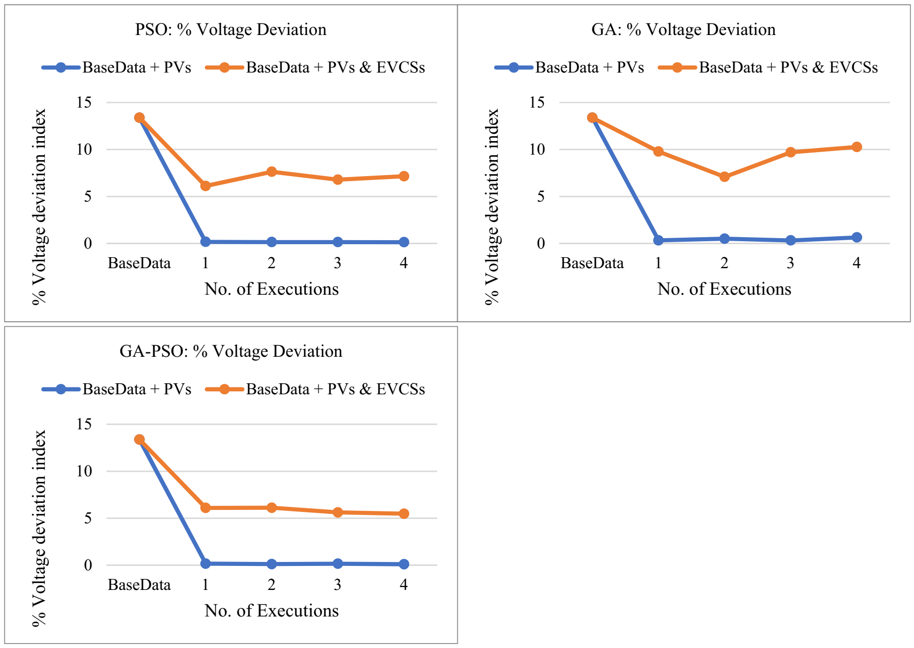

Fig. 4 Percentage voltage deviation index

Table 7 Compared network's VDI when EVCSs and random PVs are placed using PSO, GA, and hybrid GA–PSO

Base case	**Voltage deviation index under different executions (%)**		
%VDI: 13.3808	**PSO**	**GA**	**GA_PSO**
Execution-1	6.1181	9.7866	6.1086
Execution-2	7.636	7.0918	6.1221
Execution-3	6.7933	9.7066	5.6289
Execution-4	7.1577	10.2726	5.4867
Min VDI	6.1181	7.0918	5.4867

0.89494 p.u. and 0.92233 p.u., respectively. These findings highlight the superior performance of the hybrid GA–PSO algorithm in maintaining a favorable voltage profile within the network.

Based on the findings presented in Table 6, it is evident that the voltage profile of the network significantly improves when EVCSs are placed using the hybrid GA–PSO approach compared to the individual GA and PSO algorithm. Across all four execution instances, the network demonstrates better voltage performance when the EVCSs are positioned using the hybrid GA–PSO approach. Specifically, when the suggested hybrid GA–PSO approach is utilized for EVCS placement, the minimum node voltage is recorded at 0.92214 p.u. This value is higher than the minimum node voltages achieved using the GA (0.89494 p.u.) and the PSO algorithm (0.90792 p.u.). These results highlight the superior effectiveness of the hybrid GA–PSO approach in maintaining higher voltage levels within the network.

Voltage deviation index (VDI)

The voltage deviation index (VDI) serves as an indicator of the variation between a bus voltage and the reference voltage, typically set at 1 per unit (p.u.). A lower VDI value indicates that the bus voltage is closer to the reference voltage, while a higher VDI signifies a greater deviation from the reference voltage and potential concerns regarding voltage stability. In all execution instances and across all three algorithms, a significant reduction in VDI is observed with a 35% penetration of PV systems. This indicates that the bus voltages are closer to the reference voltage, indicating improved voltage stability. Figure 4 demonstrates that the introduction of EVCSs has minimal impact on the network's VDI in all execution instances. However, the

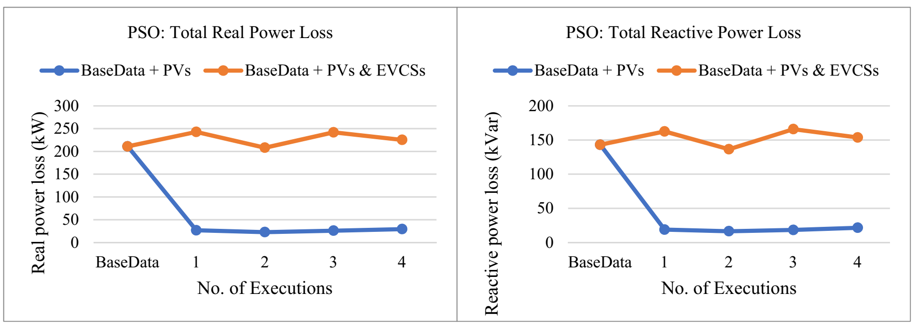

Fig. 5 PSO: total power losses

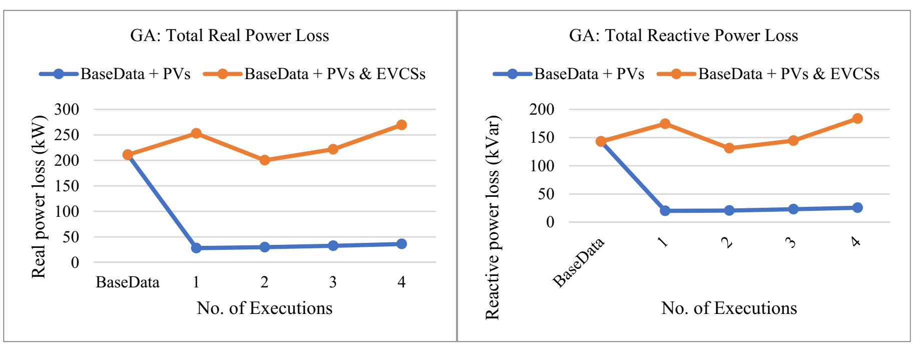

Fig. 6 GA: total power losses

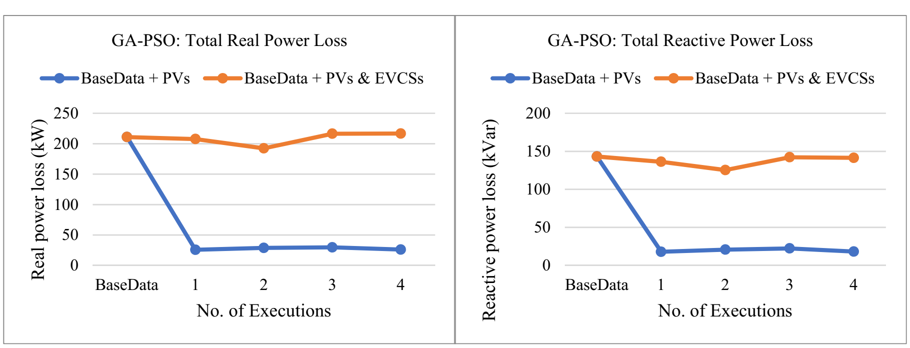

Fig. 7 GA–PSO: total power losses

Table 8 Compared network's power losses when EVCSs and PVs are placed using PSO, GA, and hybrid GA–PSO

Base case	**Total power losses under different executions**					
***P* (kW): 210.9876**	**PSO**		**GA**		**GA–PSO**	
***Q* (kVar): 143.1284**	***P* (kW)**	***Q* (kVar)**	***P* (kW)**	***Q* (kVar)**	***P* (kW)**	***Q* (kVar)**
Execution-1	242.8084	162.5749	252.9438	174.4537	207.7332	136.2307
Execution-2	208.1206	136.4967	200.2578	131.1239	192.4145	125.3715
Execution-3	241.8629	165.9052	221.7523	144.6374	216.4107	142.2413
Execution-4	225.2834	153.7716	269.4463	183.6445	216.7633	141.4762
Minimum losses	208.1206	136.4967	200.2578	131.1239	192.4145	125.3715

installation of EVCSs resulted in a rise in network VDI since the EVCS acts as additional loads to the network.

When the EVCSs are allocated using the hybrid GA–PSO, the best case of the network's percentage VDI is 5.4867%, as seen in Table 7 compared to GA and PSO that yielded 7.0918% and 6.11815% as their individual best values as percentage VDI. This indicates that utilizing hybridization procedures of GA–PSO to place the EVCSs resulted in an improved network voltage profile which is better than when GA and PSO are used alone. As a consequence of using the hybrid strategy to install the EVCSs, the network has higher-voltage stability.

Network real and reactive power losses

The influence of PV systems on total real and reactive power losses is evident in Figs. 5, 6 and 7. In comparison with the original base case values of 210.99 kW for total real power loss and 143.123 kVar for total reactive power loss, the utilization of PV systems results in a significant reduction in both parameters across all three algorithms. However, the strategic placement of EVCSs does lead to a slight increase in total real and reactive power losses. This can be attributed to the additional stress exerted on the network by the EVCSs. Nevertheless, when considering the optimal scenario outlined in Table 8, it is noteworthy that the real and reactive power losses induced by the EVCSs remain lower than those observed in the base scenario for all algorithms.

Table 8 reveals that the network's total real and reactive power losses differ when EVCSs are placed using the hybrid GA–PSO technique compared to the separate PSO and GA techniques. Specifically, the total real and reactive power losses incurred when utilizing the proposed GA–PSO technique for EVCS placement are consistently lower across all execution instances compared to the individual GA and PSO approaches.

Validation of hybrid GA–PSO over separate GA and PSO

The optimal placement of EVCSs in a radial distribution network, considering randomly sized and placed distributed PV systems, demonstrates the superiority of the hybrid GA–PSO technique over individual GA and PSO techniques. Comparative analysis of Tables 6, 7, and 8, which examine the minimum and maximum bus voltages, VDI, and total real and reactive power losses, clearly illustrates that the proposed GA–PSO technique consistently achieves superior results compared to using GA or PSO individually.

Notably, previous studies such as [16, 17] have addressed similar problems but with different considerations.

In [16], the problem of EVCS placement in a distribution network with randomly placed rooftop PVs was tackled using the hybrid BFOA-PSO technique. However, this approach did not account for the reactive power influence of PV inverters, which affects voltage and power losses. Additionally, the distribution network's load sparsity was not considered, potentially leading to local convergence of multiple EVCSs at specific buses during implementation. In [17], the authors employed the hybrid GA–PSO technique, considering the reactive nature of PV inverters and their impact on the distribution network. Nevertheless, the load density of different parts of the network was not taken into account, potentially resulting in local convergence of multiple EVCSs at specific buses during implementation.

The simulation results highlight the effectiveness of the hybrid GA–PSO technique as an optimization strategy for EVCS deployment in existing distribution networks with randomly scattered PV systems. This technique proves valuable for distribution service operators aiming to provide cost-effective and reliable services while maintaining appropriate power quality and voltage within specified limits. Furthermore, the hybrid GA–PSO technique's utility is evident in both current and future contexts. By leveraging the strengths of one algorithm to address the weaknesses of the other, the hybrid GA–PSO technique demonstrates its capability. The comparative analysis of results obtained from GA, PSO, and hybrid GA–PSO techniques provides valuable insights into their relative effectiveness as well as the edge that a hybrid metaheuristic technique has over an individual optimization. This research contributes to the understanding of EV utilization in radial distribution networks, offering practical guidance for optimizing EVCS placement, reducing power losses, and improving voltage performance. The strength of the presented results is further supported by referencing related works in the current literature, highlighting the advancements made in the field.

Conclusion

In summary, the rapid adoption of EVs as a means to reduce greenhouse gas emissions in the transportation industry necessitates the swift upgrading of distribution networks to support a large number of charging stations. The integration of EV technology also requires measures to address resource allocation challenges. This study employed metaheuristic techniques, including GA, PSO, and hybrid GA–PSO, to optimize the placement of EV charging stations (EVCSs) in a network with randomly sized and distributed PV systems. The objective function focused on minimizing real and reactive power losses and voltage deviation index. Comparative analysis revealed that the hybrid GA–PSO approach outperformed individual GA and PSO methods, achieving the lowest values of real and reactive power losses and exhibiting robustness in affecting the voltage profile. The optimal node placement for EVCSs in each zone was determined using the hybrid GA–PSO technique.

Simulation results demonstrated the effectiveness of the hybrid GA–PSO in locating suitable nodes for EVCS installation, resulting in improved real and reactive power losses, minimum network node voltage, and voltage deviation index compared to individual GA and PSO approaches. The comparative findings of the optimization methods revealed that the hybrid GA–PSO offered the lowest value of real and reactive power losses, which were 192.4145 kW and 125.3715kVar, respectively, compared to GA's real and reactive power losses of 200.2578 kW and 131.1239kVar, respectively, and PSO's real and reactive power losses of 208.1206 kW 136.4967kVar. Hybrid GA–PSO also showed superiority by affecting the voltage profile by a percentage VDI of 5.4867% on EVCS integration compared to a percentage VDI of 7.0918% and 6.1181% of GA and PSO, respectively. The hybrid GA–PSO technique was used to find the optimal solution as it was able to place four level 1 EV chargers at bus numbers 5, 9, 15, and 22 (respectively, in zone 1, zone 2, zone 3, and zone 4) and three level 2 EV chargers at bus number 25, 27, 32 (respectively, for zone 5, zone 6, and zone 7).

The study's findings contribute valuable insights and guidance for the seamless integration of EVs into radial distribution network systems that are segmented into zones. The hybrid GA–PSO approach employed in this research provides a powerful optimization framework for addressing the placement problem of EVCSs. By combining the strengths of GA and PSO, the hybrid approach enables a balance between exploration and exploitation, leading to enhanced performance in finding optimal solutions. The study's outcomes offer practical implications for policymakers, system planners, and researchers involved in the efficient deployment and management of EV charging infrastructure within community-based distribution networks. In future research, an important aspect will be the consideration of factors such as battery charge levels and the intermittent behavior of distributed PV systems. By accounting for battery charge levels, the research will be aimed at ensuring the efficient utilization of available energy resources and managing the charging demands of EVs effectively as the current work fails to take this in to account. Additionally, the intermittent nature of distributed PV systems will be taken into account to leverage renewable energy sources and maximize their integration with the EV charging infrastructure since this work had assumed the PVs were operation at their peaks.

Abbreviations

BFOA–PSO	Bacterial foraging optimization algorithm–particle swarm optimization
CP	Charging point
CS	Charging station
DG	Distributed generator
EV	Electric vehicle
EVCS	Electric vehicle charging station
GA	Genetic Algorithm
GA–PSO	Genetic algorithm–particle swarm optimization
IEEE	Institute of Electrical and Electronics Engineers
PSACO	Particle swarm ant colony optimization
PSO	Particle swarm optimization
PV	Photovoltaic
RDNS	Radial distribution network system
VDI	Voltage deviation index

Acknowledgements
This investigation did not receive any particular grant from any of the funding bodies that are located in the public, commercial, or non-profit sectors.

Author contribution
EAR contributed to the investigation, data curation, establishing methodology, and formal analysis and is major contributors to writing the manuscript. WSTF contributed to the investigation, validated the resources, and was a major contributor in reviewing and editing the manuscript. The manuscript was read and approved by all authors.

Funding
This work did not receive any funding support.

Data availability
Data included in article/supplementary material/referenced in the article.

Declarations

Consent for publication
Not applicable.

Competing interests
The authors declare no conflict of interest.

Received: 25 May 2023 Accepted: 20 November 2023
Published online: 02 January 2024

References

1. Fuinhas JA, Koengkan M, Leitão NC, Nwani C, Uzuner G, Dehdar F, Relva S, Peyerl D (2021) Effect of battery electric vehicles on greenhouse gas emissions in 29 European Union countries. Sustainability 13:13611
2. Yong JY, Ramachandaramurthy VK, Tan KM, Mithulananthan N (2015) A review on the state-of-the-art technologies of the electric vehicle, its impacts and prospects. Renew Sustain Energy Rev 49:365–385
3. Li Z, Khajepour A, Song J (2019) A comprehensive review of the key technologies for pure electric vehicles. Energy 182:824–883
4. Rubino L, Capasso C, Veneri O (2017) Review on plug-in electric vehicle charging architectures integrated with distributed energy sources for sustainable mobility. Appl Energy 207:438–464
5. Du J, Liu Y, Mo X, Li Y, Li J, Wu X, Ouyang M (2019) Impact of high-power charging on the durability and safety of lithium batteries used in long-range battery electric vehicles. Appl Energy 255:113793
6. Lulhe AM, Date TN (2015) A technology review paper for drives used in the electrical vehicle (EV) & hybrid electrical vehicles (HEV). In: Proceedings of the 2015 international conference on control, instrumentation, communication and computational technologies (ICCICCT), Kumaracoil, India, 18–19 December
7. Clement-Nyns K, Haesen E, Driesen J (2010) The impact of charging plug-in hybrid electric vehicles on a residential distribution grid. IEEE Trans Power Syst 25:371–380
8. Qazi HW, Flynn D, Rather ZH (2016) Impact of electric vehicle load response variation on frequency stability. In: 2016 IEEE PES innovative smart grid technologies conference Europe (ISGTEurope)
9. Kim M, Kim J, Bae S (2016) Design of a sustainable and efficient transportation station (SETS) based on renewable sources and efficient electric drives. Symmetry 8:146
10. Kijewska A, Bluszcz A (2016) Analysis of greenhouse gas emissions in the European Union member states with the use of an agglomeration algorithm. J Sustain Min 15:133–142
11. Ahmadi L, Croiset E, Elkamel A, Douglas P, Unbangluang W, Entchev E (2012) Impact of PHEVs penetration on Ontario's electricity grid and environmental considerations. Energies 5:5019
12. Sadhukhan A, Sivasubramani S, Ahmad MS (2019) Optimal placement of electric vehicle charging stations in a distribution network. In: 8th international conference on power systems (ICPS). IEEE
13. Mohan B, Ramesh MV (2012) Optimal DG placement under Standard Market Design using GA. In: Proceedings of the 2012 international conference on emerging trends in electrical engineering and energy management (ICETEEEM), Tamil Nadu, India, 13–15 December
14. Rene EA, Fokui WST (2023) A quantum particle swarm optimization-based optimal LQR-PID controller for load frequency control of an isolated power system. J Eng Appl Sci 70:97
15. El-Zonkoly A (2011) Optimal placement of multi-distributed generation units including different load models using particle swarm optimization. Swarm Evol Comput 1:50–59
16. Fokui WST, Saulo MJ, Ngoo L (2021) Optimal placement of electric vehicle charging stations in a distribution network with randomly distributed rooftop photovoltaic systems. IEEE Access 9:132397–132411
17. Rene EA, Fokui WST, Kouonchie PKN (2023) Optimal allocation of plug-in electric vehicle charging stations in the distribution network with distributed generation. Green Energy Intell Transp 2:100094
18. Babu PVK, Swarnasri K, Vijetha P (2018) A three phase unbalanced power flow method for secondary distribution system. Adv Model Anal B 61:139–144
19. Kashem MA, Ganapathy V, Jasmon GB, Buhari MI (2000) A novel method for loss minimization in distribution networks. In: Proceedings of the international conference on electric utility deregulation and restructuring and power technologies, London, UK, pp 251–256, 4–7 April
20. Mohanty AK, Babu PS, Salkuti SR (2022) Fuzzy-based simultaneous optimal placement of electric vehicle charging stations, distributed generators, and DSTATCOM in a distribution system. Energies 15:8702
21. Pande S, Ghodekar JG (2012) Computation of technical power loss of feeders and transformers in distribution system using load factor and load loss factor. Int J Multidiscip Sci Eng 3:22–25
22. Yenchamchalit K, Kongjeen Y, Prabpal P, Bhumkittipich K (2021) Optimal placement of distributed photovoltaic systems and electric vehicle charging stations using metaheuristic optimization techniques. Symmetry 13:2378
23. Arumugam MS, Rao MVC (2008) On the improved performances of the particle swarm optimization algorithms with adaptive parameters, cross-over operators and root mean square (RMS) variants for computing optimal control of a class of hybrid systems. Appl Soft Comput 8:324–336
24. Kachitvichyanukul V (2008) Recent advances in adaptive particle swarm optimization algorithms. In: 대한산업공학회 추계학술대회 논문집
25. Goldberg DE (1989) Genetic algorithms in search, optimization and machine learning. Addison-Wesley, Reading

26. Suyanto A (2005) Algoritma Genetika dalam MATLAB. Andi, Yogyakarta
27. Shelokar PS, Siarry P, Jayaraman VK, Kulkarni BD (2007) Particle swarm and ant colony algorithms hybridized for improved continuous optimization. Appl Math Comput 188:129–142
28. Kao Y-T, Zahara E (2008) A hybrid genetic algorithm and particle swarm optimization for multimodal functions. Appl Soft Comput 8:849–857
29. Voratas K (2012) Comparison of three evolutionary algorithms: GA, PSO, and DE. Ind Eng Manag Syst 11:215–223
30. Hook JV, Sahin F, Arnavut Z (2008) Application of particle swarm optimization for traveling salesman problem to lossless compression of color palette images. In: IEEE international conference on system of systems engineering, Monterey, CA, USA, 02–04 June
31. Zhang Y, Gong DW, Cheng J (2017) Multi-objective particle swarm optimization approach for cost-based feature selection in classification. IEEE/ACM Trans Comput Biol Bioinform 14:64–75
32. Turney PD (1995) Cost-sensitive classification: empirical evaluation of a hybrid genetic decision tree induction algorithm. J Artif Intell Res 2:41
33. Min F, Hu Q, Zhu W (2014) Feature selection with test cost constraint. Int J Approx Reason 55:167–179
34. Haralick RM, Shanmugam K, Dinstein I (1973) Textural features for image classification. IEEE Trans Syst Man Cybern SMC-3:610–662

Publisher's Note

Springer Nature remains neutral with regard to jurisdictional claims in published maps and institutional affiliations.